Advances in Clinical and Experimental Dentistry

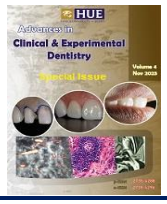

Research Article

Fluorescence in situ hybridization probes will not be used in diagnosing maxillofacial lesion sooner than 2030: A time-series analysis

Ebraheme Boceila[1], MSc , Myye Wafeqe[1], MSc, and BacemA. Khalele[2], MSc

Abstract

Background Fluorescence in situ hybridization (FISH) is highly accurate in detecting specific genetic rearrangements or gene amplifications. It provides direct visualization of chromosomal abnormalities or gene fusions at the cellular level.

Objective This article investigated the molecular labeling of maxillofacial lesions and examined the detectable genetic alterations using FISH analysis. The study discussed the merits and limits of FISH analysis in diagnosing these lesions and provided insights into the future applicability of FISH as a diagnostic tool.

Method We conducted a comprehensive search of electronic databases (e.g., PubMed, Embase, Web of Science) to identify relevant studies published within a specific time frame. We utilized appropriate search terms, including "maxillofacial lesions," "fluorescence in situ hybridization," "genetic alterations," "diagnosis," and related keywords .Included articles published in English, targeting human subjects, and focused on the molecular characterization of maxillofacial lesions using FISH analysis. Iterative refinement and validation were used for improving the accuracy of predictions of the timeseries analysis.

Results We identified the limitations and challenges associated with FISH analysis in maxillofacial lesions, such as the non-specificity of genetic alterations and the limited availability of fusion probes. We analyzed the implications of these findings and inferred the future applicability of FISH analysis in the diagnosis of maxillofacial lesions.

Advances in Knowledge The evolving landscape of molecular diagnostic techniques uses more trendy and efficient techniques than FISH analysis. With competing such techniques, FISH is less likely to be of use soon unless promising avenues are to be proposed for overcoming existing limitations.

Keywords: FISH, Maxillofacial, Salivary neoplasms, Sinonasal, Odontogenic, Molecular

1 . Ministry of Health, Egypt **2** .Department of Oral Pathology, Mansoura University, Egypt (Corresponding author)
Email: bkhalele@horus.edu.eg
DOI: 10.21608/ACED.2023.249282.1024

Introduction

Fluorescence in situ hybridization (FISH) offers direct visualization of abnormalities in chromosomes or fused genes within cells, enabling the precise pinpointing of distinct genetic changes. FISH probes commonly used in maxillofacial molecular diagnosis include fusion probes and break-apart FISH probes, which offer several advantages and demonstrate superiority in certain diagnostic applications. Break-apart FISH probes are specifically designed to detect genetic rearrangements in target genes, such as translocations, inversions, or deletions. These rearrangements can be critical diagnostic markers for diagnostically challenging neoplasms by identifying the presence of gene rearrangements[1,2].

Break-apart FISH probes are designed to hybridize to adjacent regions on either side of the breakpoint in the target gene. If a rearrangement has occurred, the signals from the two probe regions will be separated, typically use different fluorophores or colors for the two probe regions, indicating the presence of the rearrangement. When the gene is intact, the probes will be close together, showing a fused or overlapping signal. The probes will be separated in rearrangement, leading to distinct split or separate signals. The extent of the rearrangement can be determined by assessing the percentage of cells with split signals or calculating the ratio of split signals to fused signals. This quantitative approach provides additional information about the disease and can be helpful in prognosis and treatment decisions. This visual differentiation enhances the interpretation of results and facilitates the identification of genetic rearrangements[3].

However, if a novel or unknown rearrangement occurs in the gene of interest, break-apart FISH probes may not be able to detect it. These probes are only effective when the target rearrangement is already characterized and incorporated into the probe design. FISH probes may also fail to detect specific rearrangements that involve alterations in the probe binding regions. If a rearrangement disrupts or deletes one or both binding sites, the probes may not be able to hybridize appropriately, resulting in false negative results. Therefore, break apart. Break-apart FISH probes can detect the presence of a genetic rearrangement but do not provide information about the specific fusion partner involved. In some cases, fusion FISH probes are commercially available. If not, reverse transcription polymerase chain reaction (RTPCR) or next-generation sequencing (NGS) will be required to determine the fusion partner gene to encode the underlying oncogenesis of the rearrangement and may have implications for targeted therapies. RTPCR is a sensitive and specific technique for detecting gene expression levels and gene fusions. It can quantify RNA transcripts and identify specific fusion events with high accuracy. It is limited to known fusion partners and, requires prior knowledge of the target genes involved in the fusion and susceptible to false negatives due to variations in RNA quality or quantity, and it may not provide information on genomic structural variants or mutations outside the known fusion sites. NGS offers high accuracy and comprehensive genomic profiling. It can detect various genetic alterations, including point mutations, insertions/deletions, gene fusions, and copy number variations. NGS provides a detailed

view of the entire genome or targeted gene panel, enabling a comprehensive analysis of genetic changes. However, NGS requires advanced bioinformatics analysis and expertise to interpret the data generated. It may have limitations in detecting low-level mutations or rare genetic alterations depending on the depth of sequencing coverage. NGS can be more expensive and time-consuming compared to other techniques, and it may not be necessary for routine diagnosis unless a comprehensive genomic assessment is required.

Method

First, PubMed, Embase, and Web of Science were searched for maxillofacial articles that used FISH analysis as a molecular tool to verify the diagnosis of maxillofacial lesions. These databases were chosen for their extensive coverage of scientific literature across various disciplines.

We then employed appropriate search terms that encompassed the key aspects of our study. The search terms included "maxillofacial lesions," "fluorescence in situ hybridization," "genetic alterations," "diagnosis," and other related keywords. By combining these terms using Boolean operators (e.g., AND, OR), we refined our search and ensured a comprehensive coverage of the topic.

To narrow down the search results and maintain a focus on human subjects, we applied filters to include only articles published in English and targeting human populations. This helped us eliminate studies conducted on animals or in vitro models, ensuring the relevance and applicability of the findings to our study objective.

After retrieving the articles, we carefully screened their titles and abstracts to determine their suitability for inclusion. We assessed whether they met our criteria of focusing on the molecular characterization of maxillofacial lesions using FISH analysis. Studies that met these criteria were selected for further evaluation.

The selected articles were then thoroughly analyzed, and the data extracted from each study were organized systematically. We categorized the findings based on the specific genetic alterations detected by FISH analysis in maxillofacial lesions. Key outcomes and significant observations were highlighted to provide a comprehensive overview of the current knowledge in the field.

With the data organized, we examined the specificity, and sensitivity of each FISH probe and their ability to detect specific genetic alterations that are associated with these lesions.

Time Series Analysis

We loaded the "forecast" library, which provided functions for time series analysis and forecasting. The data representing FISH usage from 2010 to 2022 was converted into a time series object using the *ts* function. The data argument contained the FISH usage values, and the start argument specified the starting year of the time series. The frequency was set to 1 since the data was annual (recorded once per year). A simple line plot of the FISH usage over the years was created using the plot function. This plot gave a visual

overview of the data and allowed us to identify any apparent trends or patterns. The decompose function separated the time series into its constituent components: trend, seasonality, and residuals (error term). This decomposition helped in understanding the underlying patterns in the data. Stationarity was an essential assumption for ARIMA modeling. If the time series was found to be nonstationary (i.e., the mean, variance, or autocorrelation structure changed over time), differencing might have been applied to make it stationary. The *auto.arima* function was employed to automatically select the best ARIMA model based on the data's characteristics and the AIC value. The Akaike Information Criterion (AIC) measured the model's goodness of fit while penalizing for complexity. The summary of the fitted ARIMA model was printed, which provided information about the model's order (p, d, q) and coefficients.

Two evaluation criteria, the Akaike information criterion (AIC) and the normalized root mean square error (NRMSE), were used to assess and compare different models. The AIC was employed to select the most suitable statistical model from competing ones, preferring the model with the lowest AIC value. Its calculation involved considering the number of parameters (k), the total data points (N), and the loss function (I) for the predicted function.

The AIC can be computed as AIC = 2k 2ln(I), where k represents the number of model parameters, N is the number of data points, and I is the loss function value. The NRMSE served as a measure of modeling accuracy, evaluating and comparing model performance in predicting data. It quantified the consistency between estimated and actual data. To calculate NRMSE, the Euclidean norm between the vector of real values (Xtarget) and the vector of estimated values (Xpredicted) was normalized by the Euclidean norm between the vector of real values and their mean (Xmean).

$NRMSE = \|Xtarget\ Xpredicted\|_2 / \|Xtarget\ Xmean\|_2$, *where Xtarget is the vector of real values, Xpredicted is the vector of estimated values, and* $\|...\|_2$ *denotes the Euclidean norm.*

The models used for this analysis were "AutoRegressive Moving Average" (ARMA) models, and the identification and predictions were performed using the Matlab System Identification Toolbox. Using the fitted ARIMA model, the forecast function was used to make predictions for the next 10 years (2023 to 2033). The h argument in the forecast function specified the number of periods (years) for which we wanted to make predictions. A plot of the forecasted FISH usage from 2023 to 2033 was created using the plot function. This plot displayed the forecasted values along with uncertainty intervals.

Results

The most frequently reported diagnostic genes in maxillofacial pathology are *EWSR1*, *MAML2*, *ALK, USP6, PLAG1, FUS, NTRK3, NTRK1, HMGA2, BRAF, YAP1, MYB and NR4A3*. Recently, *SS18, RET, NUTM1, TFE3, CIC, DEK, AFF2*, and *KMT2A* have been linked to emerging neoplasms with aggressive clinical course (Table 1).

Table 1. Frequently used FISH probes in diagnosing maxillofacial lesions.

Gene	Frequently altered in
AFF2	
ALK	Adenocarcinoma with EML4::ALK fusion
BRAF	Solitary fibrous tumor (*BBS9::BRAF*); Myxoinflammatory fibroblastic sarcoma (*SND1::BRAF*, *TOM1L2::BRAF*); Ameloblastoma
CIC	*CIC::DUX4* fusion associated with undifferentiated round cell sarcoma
DEK	Sinonasal squamous cell carcinoma (*DEK::AFF2*); Acute myeloid leukemias, myelodysplastic syndromes
EWSR1	Desmoplastic small round cell tumor (*EWSR1::WT1*); Ewing sarcoma (*EWSR1::ERG*, *EWSR1::FEV*); Myoepitheliomatous neoplasms and myxofibrosarcoma (*EWSR1::PBX1*); Embryonal rhabdomyosarcoma and Giant cell tumor of bone (*EWSR1::FLI1*); Clear cell sarcoma (*EWSR1::ATF1*, *EWSR1::CREM*); Hyalinizing clear cell carcinoma (*EWSR1::ATF1*)
FUS	Ewing sarcoma (*FUS::FEV*, *FUS::ERG*)
KMT2A	Leukemia
MAML2	Mucoepidermoid Carcinoma
MYB	Adenoid cystic carcinoma
NR4A3	Chondrosarcoma, myxoid (*SMARCA2::NR4A3*, *TFG::NR4A3*, *FUS::NR4A3*, *TAF15::NR4A3*, *EWSR1::NR4A3*, *HSPA8::NR4A3*); Osteosarcoma, NOS
NTRK1/3	Infantile fibrosarcoma (*ETV6::NTRK3*, *LMNA::NTRK1*) Mammary Analog Secretory Carcinoma (*ETV6::NTRK3)*
NUTM1	NUT Carcinoma
PLAG1	Lipoblastomas and salivary gland mixed neoplasms and other epitheloid malignancies
RET	Intraductal Carcinoma (*NCOA4::RET*, *TRIM27::RET*)
SS18	Epithelioid sarcoma/Synovial sarcoma (*SS18L1::SSX1*, *CRTC1::SS18*, *SS18::ZBTB7A*, *SS18::SSX1*); Undifferentiated round cell sarcoma; Microcribriform Adenocarcinoma of Salivary Glands(*SS18::ZBTB7A*); Microsecretory Adenocarcinoma (*MEF2C::SS18*)
TFE3	PEComa (*SFPQ::TFE3*, *RBMX::TFE3*, *NONO::TFE3*, *SFPQ::TFE3*, *DVL2::TFE3*); Alveolar soft part sarcoma (*DVL2::TFE3*, *PRCC::TFE3*); Ossifying fibromyxoid tumor (*PHF1::TFE3*)
USP6	Aneurysmal bone cyst (*LUM::USP6*, *OMD::USP6*, *USP6::LUM*, *EIF1::USP6*, *VDR::USP6*); Nodular fasciitis (*MYH9::USP6*)
YAP1	Spindle cell/sclerosing rhabdomyosarcoma; Squamoid Porocarcinoma (*YAP1::MAML2*)

To visualize the usage from 2010 to 2022, a simple line plot displays the FISH usage from 2010 to 2022 (Figure 1). The x-axis represents the years, and the y-axis represents the FISH usage values. Each data point on the plot corresponds to the FISH usage in a specific year. The line connects these data points to show the trend in FISH usage over the observed period.

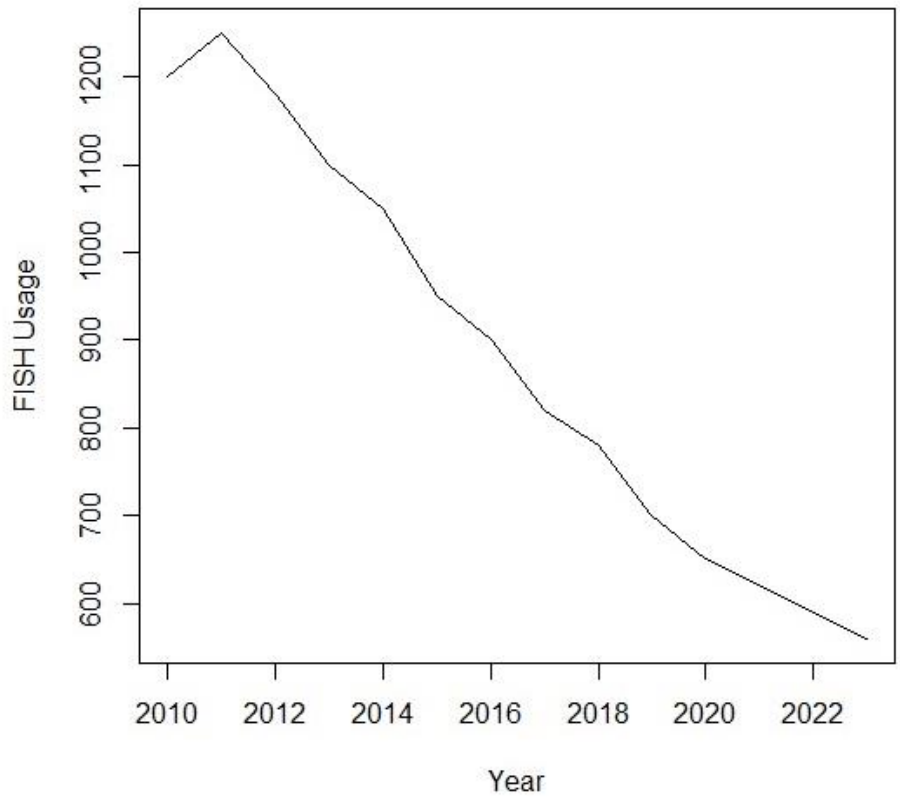

Figure 1. FISH usage from 2010 to 2022

The decomposition dissects the original time series data, representing FISH usage, into three fundamental components. First and foremost, the trend component unveils the enduring movement or trajectory of FISH usage over the years, providing valuable insights into the overarching direction of change, be it a gradual increase or a steady decline. Secondly, the seasonal component captures the patterns and oscillations that emerge at fixed intervals, needed to discern periodic variations in FISH usage that persistently manifest over time. Lastly, the Residual (Error) component encompasses the fluctuations and random noise that elude explanation from both the trend and seasonal aspects. It accounts for the unpredictable variability in FISH usage that defies the grasp of the model.

By scrutinizing these three components, we gain a profound comprehension of the underlying structures woven within the data. This scrutiny allows us to detect noteworthy trends, ascertain the presence of seasonality, and identify any exceptional deviations in FISH usage. Such decomposition proves invaluable as it validates the suitability of employing an ARIMA model for precise forecasting while illuminating the sources of variation present in the time series data.

The algorithm predicted the value of a time series at a specific time point using a combination of past observations, gradients, and previous predictions. The parameters α and β were optimized through an external optimization function $fit()$, which updated these parameters based on past observations ($\alpha t-1$ and $\beta t-1$) and the input time series [$X1…Xt$] with the learning rate η.

 DOI: 10.21608/ACED.2023.249282.1024

The algorithm looped through the time series from time $T1$ to $T-1$ (exclusive), where T was the total length of the time series.

For each time point (t), the algorithm predicted the value of the time series at that point, denoted as $X\tilde{}t(\alpha, \beta)$. The prediction $X\tilde{}t(\alpha, \beta)$ was composed of three components:

a. $\sum d-1i=0\nabla iXt-1$: This part captured the past observations up to $d1$ time points before t.

b. $\sum qi=1\beta i\epsilon t-i$: This part involved the previous q predictions, weighted by the β coefficients and the threshold $\epsilon t-i$.

c. $\sum pi=1\alpha i\nabla dXt-i$: This part captured the past p gradients, weighted by the α coefficients.

A constant value c was added to the prediction $X\tilde{}t(\alpha, \beta)$. The algorithm checked if the absolute difference between the predicted value $X\tilde{}t$ and the actual value Xt at time t was less than the threshold $\epsilon th\tilde{}$. If the condition $|X\tilde{}t-Xt| < \epsilon th\tilde{}$ was met, it meant the prediction was accurate enough, and the algorithm considered the time point t as a suitable prediction. Thus, the value of t was added to the list r. The ALERT step could have been a notification mechanism indicating that the one-point prediction for time t was successful. The algorithm continued the loop for all time points in the time series.

Discussion

Given the availability of very limited commercial fusion probes, the use of break-apart probe is no longer helpful diagnostically or prognostically. For example, the *EWSR1* gene partners with more than ten genes in maxillofacial lesions. Desmoplastic small round cell tumor[4,5] is characterized by nests, cords, or sheets of small round cells embedded in a desmoplastic stroma. The tumor cells typically have a high nuclear-to-cytoplasmic ratio, prominent nucleoli, and a characteristic desmoplastic reaction. It harbors the fusion of *EWSR1* gene with the WT1 gene. Ewing sarcoma is composed of small round cells with uniform round nuclei and scant cytoplasm. The densely packed cells may form rosette-like structures (HomerWright rosettes) or sheets. The tumor cells often show a high mitotic rate and areas of necrosis. It is associated with several fusion variants, including *EWSR1*::ERG[6–9] and *EWSR1*::FEV[6,10]. These translocations involve the fusion of the *EWSR1* gene with the ERG or FEV gene. Both myoepitheliomatous neoplasms and myxofibrosarcoma can exhibit *EWSR1* gene translocation with the PBX1 gene[11]. Myoepitheliomatous neoplasms typically show a biphasic growth pattern consisting of both epithelioid and spindle cell components. The tumor cells may exhibit clear cytoplasm and show myoepithelial differentiation.

Myxofibrosarcoma is characterized by a predominantly myxoid stroma with scattered spindle-shaped tumor cells. The tumor cells have elongated nuclei, moderate cytoplasm, and variable degrees of pleomorphism. Myxofibrosarcoma shows infiltrative growth and a multinodular growth pattern[12]. Embryonal rhabdomyosarcoma and Giant cell tumor of bone are associated with the fusion of *EWSR1* gene with the FLI1 gene. Embryonal rhabdomyosarcoma comprises primitive mesenchymal cells that differentiate into various stages of skeletal muscle development. The tumor cells may form embryonal or straplike rhabdomyoblasts, elongated cells with eosinophilic cytoplasm and cross-striation. However, giant cell tumor of bone is characterized by

multinucleated osteoclast-like giant cells dispersed within a background of mononuclear spindle-shaped or round tumor cells. The tumor cells have a bland appearance with oval to elongated nuclei and variable amounts of cytoplasm. Areas of hemorrhage and osteoid formation may also be observed[13]. Moreover, clear cell sarcoma can present with *EWSR1* gene translocation involving either the ATF1 or CREM gene[14,15]. Clear cell sarcoma is characterized by nests or sheets of epithelioid or spindled tumor with clear to eosinophilic cytoplasm. The tumor cells typically have round to oval nuclei and may show prominent nucleoli.

The presence of melanin pigment is a characteristic feature, and the tumor cells may also exhibit a fascicular growth pattern. Hyalinizing clear cell carcinoma (HCCC) is an *EWSR1*-rearranged salivary gland tumor characterized by a solid, nested, or trabecular growth pattern of neoplastic cells with abundant clear cytoplasm. The cytoplasmic clearing is caused by the accumulation of glycogen and lipid droplets, giving the cells a clear or eosinophilic appearance. The tumor cells of HCCC are polygonal to round and have centrally located nuclei. The nuclei are usually round or ovoid, with finely dispersed chromatin and small nucleoli. Nuclear atypia and mitotic activity may vary but are generally low. The hyalinized stroma appears as eosinophilic material between the tumor cell nests[16–20]. Equivalently, clear cell odontogenic tumor is believed to be the intraosseous counterpart of HCCC, which shows similar molecular and histologic profile[21,22]. Obviously, the *EWSR1*maxillofacial neoplasms show a heterogenous morphology, which does not suffice to confer a particular oncogeneitc pathway that explain any association.

The lack of fusion diagnostic probes is not the only limitation, but significant break-apart probes, such as High Mobility Group ATHook 2 (*HMGA2*) and Pleomorphic Adenoma Gene 1 (*PLAG1*), are not available as well. *PLAG1* is frequently involved in gene fusions in pleomorphic adenoma, a common benign salivary gland tumor. *PLAG1* gene rearrangements result in the overexpression of *PLAG1* protein, which plays a role in cell proliferation and tumor development. *HMGA2* gene alteration is frequently observed in benign tumors such as lipomas and pleomorphic adenomas. Both *PLAG1* and *HMGA2* genetic alteration are evident in carcinoma ex pleomorphic adenoma.

On the other hand, the immunohistochemical availability of the antibodies corresponding to the investigated genes are effacing the need for FISH analysis. For example, the mammary analog secretory carcinoma (MASC) was introduced in 2010 [23], harboring *ETV6*::*NTRK3* fusion. With the introduction of diagnostic markers that distinguish MASC from acinic cell carcinoma (e.g. DOG1), a molecularly based IHC marker is now available for replacing molecular detection of *ETV6*::*NTRK3* fusion[24–27]. Even acinic cell carcinoma is diagnosed by immunopositivity for *NR4A3*[28–31] without establishing fusion script. Similarly, ETV4[32] suffices to diagnose CIC-rearranged sarcomas. IHC AFF2 [33] has effectively diagnosed DEK-rearranged sinonasal nonkeratinizing papillary squamous cell carcinoma. Also, IHC SS18, PRDK1 and MYB are sufficient for diagnosing salivary microsecretory Adenocarcinoma[34], polymorphous carcinoma[35], and adenoid cystic carcinoma[36–38], respectively.

Less popular is using FISH in diagnosing odontogenic lesions. Although Ubiquitin Specific Peptidase 6 (*USP6*) is sensitive in diagnosing aneurismal bone cysts[39–43], FISH analysis is not used to diagnose these cysts.

Conclusion

The availability of specific antibodies for immunohistochemical (IHC) analysis, along with their ease of use and affordability, has contributed to a reluctance to confirm diagnoses molecularly if the morphological features are straightforward. IHC allows for the detection of specific proteins or antigens that are associated with certain genetic alterations or disease processes. By staining tissue sections with specific antibodies, pathologists can observe the presence or absence of these markers, providing valuable information for diagnosis. Besides, in cases where the morphological characteristics of a lesion are clearly indicative of a specific diagnosis, there may be less motivation to pursue further molecular testing. Morphology refers to the microscopic appearance of cells and tissues, which can often provide valuable diagnostic clues. If the morphology is highly characteristic of a particular disease entity, additional molecular testing, such as fluorescence in situ hybridization (FISH), may not be deemed necessary. Furthermore, the nonavailability of important fusion probes further hampers the application of FISH analysis. Fusion probes are specifically designed to detect specific gene fusions or rearrangements. However, the commercial availability of fusion probes is often limited, which restricts their use in routine diagnostic practice. Without access to these probes, the ability to detect and confirm specific gene fusions through FISH analysis becomes challenging.

Another factor that may diminish the future use of FISH analysis is the non-specificity of some genetic alterations. Some gene rearrangements or fusions may be observed in multiple tumor types or have limited clinical significance. In such cases, the detection of these genetic alterations by FISH may not provide definitive diagnostic or prognostic information. This non-specificity can reduce the utility of FISH as a standalone diagnostic tool. Considering these factors, the combination of readily available and cost-effective IHC analysis, the reliance on morphology for straightforward diagnoses, the non-specificity of certain genetic alterations, and the limited availability of fusion probes may diminish the prospects for FISH analysis to be extensively used in the future. However, it is important to note that FISH still holds value in certain diagnostic scenarios where it remains a reliable and specific method for detecting specific genetic alterations, especially when morphology alone is insufficient for a conclusive diagnosis.

Notes: None

Acknowledgements: None

Funding resources: None

Conflict of interest: The authors declare no conflict of interest.

References

[1] Yoshida A, Arai Y, Kobayashi E, Yonemori K, Ogura K, Hama N, et al. CIC break-apart fluorescence in-situ hybridization misses a subset of CIC–DUX4 sarcomas: a clinicopathological and molecular study. Histopathology 2017;71:461–9. https://doi.org/10.1111/his.13252.

[2] Bishop JA, Koduru P, Veremis BM, Oliai BR, Weinreb I, Rooper LM, et al. SS18 Break-Apart Fluorescence In Situ Hybridization is a Practical and Effective Method for Diagnosing Microsecretory Adenocarcinoma of Salivary Glands. Head Neck Pathol 2021;15:723–6. https://doi.org/10.1007/s12105-020-01280-7.

[3] Gozzetti A, Le Beau MM. Fluorescence in situ hybridization: Uses and limitations. Semin. Hematol., vol. 37, 2000. https://doi.org/10.1016/S0037-1963(00)90013-1.

[4] La Starza R, Barba G, Nofrini V, Pierini T, Pierini V, Marcomigni L, et al. Multiple EWSR1-WT1 and WT1-EWSR1 copies in two cases of desmoplastic round cell tumor. Cancer Genet 2013;206. https://doi.org/10.1016/j.cancergen.2013.10.005.

[5] Gedminas JM, Chasse MH, McBrairty M, Beddows I, Kitchen-Goosen SM, Grohar PJ. Desmoplastic small round cell tumor is dependent on the EWS-WT1 transcription factor. Oncogenesis 2020;9. https://doi.org/10.1038/s41389-020-0224-1.

[6] Renzi S, Anderson ND, Light N, Gupta A. Ewing-like sarcoma: An emerging family of round cell sarcomas. J Cell Physiol 2019;234:7999–8007. https://doi.org/10.1002/jcp.27558.

[7] Zhou M, Ko YCK, Charville GW, Ganjoo KN. Sinonasal FUS-ERG-Rearranged Ewing's Sarcoma Mimicking Glomangiopericytoma. Case Rep Oncol 2020;13:1393–6. https://doi.org/10.1159/000511415.

[8] Debelenko L V., McGregor LM, Shivakumar BR, Dorfman HD, Raimondi SC. A novel EWSR1-CREB3L1 fusion transcript in a case of small cell osteosarcoma. Genes Chromosom Cancer 2011;50. https://doi.org/10.1002/gcc.20923.

[9] Wang WL, Patel NR, Caragea M, Hogendoorn PCW, López-Terrada D, Hornick JL, et al. Expression of ERG, an Ets family transcription factor, identifies ERG-rearranged Ewing sarcoma. Mod Pathol 2012;25. https://doi.org/10.1038/modpathol.2012.97.

[10] Chen S, Deniz K, Sung YS, Zhang L, Dry S, Antonescu CR. Ewing sarcoma with ERG gene rearrangements: A molecular study focusing on the prevalence of FUS-ERG and common pitfalls in detecting EWSR1-ERG fusions by FISH. Genes Chromosom Cancer 2016;55:340–9. https://doi.org/10.1002/gcc.22336.

[11] Agaram NP, Chen HW, Zhang L, Sung YS, Panicek D, Healey JH, et al. EWSR1-PBX3: A novel gene fusion in myoepithelial tumors. Genes Chromosom Cancer 2015;54. https://doi.org/10.1002/gcc.22216.

[12] Downs-Kelly E, Goldblum JR, Patel RM, Weiss SW, Folpe AL, Mertens F, et al. The utility of fluorescence in situ hybridization (FISH) in the diagnosis of myxoid soft tissue neoplasms. Am J Surg Pathol 2008;32:8–13. https://doi.org/10.1097/PAS.0b013e3181578d5a.

[13] Schaefer IM, Hornick JL. Diagnostic Immunohistochemistry for Soft Tissue and Bone Tumors: An Update. Adv Anat Pathol 2018;25. https://doi.org/10.1097/PAP.0000000000000204.

[14] Thway K, Fisher C. Tumors with EWSR1-CREB1 and EWSR1-ATF1 fusions: The current status. Am J Surg Pathol 2012;36. https://doi.org/10.1097/PAS.0b013e31825485c5.

[15] Wang WL, Mayordomo E, Zhang W, Hernandez VS, Tuvin D, Garcia L, et al. Detection and characterization of EWSR1/ATF1 and EWSR1/CREB1 chimeric transcripts in clear cell sarcoma (melanoma of soft parts). Mod Pathol 2009;22:1201–9. https://doi.org/10.1038/modpathol.2009.85.

[16] Nakano T, Yamamoto H, Nishijima T, Tamiya S, Shiratsuchi H, Nakashima T, et al. Hyalinizing clear cell carcinoma with EWSR1-ATF1 fusion gene: report of three cases with molecular analyses. Virchows Arch 2015;466:37–43. https://doi.org/10.1007/s00428-014-1676-5.

[17] Skálová A, Stenman G, Simpson RHW, Hellquist H, Slouka D, Svoboda T, et al. The role of molecular testing in the differential diagnosis of salivary gland carcinomas. Am J Surg Pathol 2018;42:e11–27. https://doi.org/10.1097/PAS.0000000000000980.

[18] Hernandez–Prera JC, Kwan R, Tripodi J, Chiosea S, Cordon–Cardo C, Najfeld V, et al. Reappraising

hyalinizing clear cell carcinoma: A population-based study with molecular confirmation. Head Neck 2017;39:503–11. https://doi.org/10.1002/hed.24637.

[19] Antonescu CR, Katabi N, Zhang L, Sung YS, Seethala RR, Jordan RC, et al. EWSR1-ATF1 fusion is a novel and consistent finding in hyalinizing clear-cell carcinoma of salivary gland. Genes Chromosom Cancer 2011;50:559–70. https://doi.org/10.1002/gcc.20881.

[20] Lanic MD, Guérin R, Sater V, Durdilly P, Ruminy P, Skálová A, et al. A novel SMARCA2-CREM fusion expending the molecular spectrum of salivary gland hyalinazing clear cell carcinoma beyond the FET genes. Genes Chromosom Cancer 2023;62. https://doi.org/10.1002/gcc.23114.

[21] Guastaldi F, Faquin W, Rivera M, Gootkind F, Hashemi S, August M, et al. Clear cell odontogenic carcinoma: a rare jaw tumor. a review of 107 cases. Int J Oral Maxillofac Surg 2019;48:93–4. https://doi.org/10.1016/j.ijom.2019.03.284.

[22] Xie R, Wang W, Thomas AM, Li S, Qin H. Maxillary clear cell odontogenic carcinoma with EWSR1-ATF1 fusion gene mimicking sclerosing odontogenic carcinoma: A case report and literature review. Pathol Res Pract 2023;241. https://doi.org/10.1016/j.prp.2022.154257.

[23] Skálová A, Vanecek T, Sima R, Laco J, Weinreb I, Perez-Ordonez B, et al. Mammary analogue secretory carcinoma of salivary glands, containing the etv6-ntrk3 fusion gene: A hitherto undescribed salivary gland tumor entity. Am J Surg Pathol 2010;34:599–608. https://doi.org/10.1097/PAS.0b013e3181d9efcc.

[24] Csanyi-Bastien M, Lanic MD, Beaussire L, Ferric S, Franc¸ois A, Meseure D, et al. Pan-TRK Immunohistochemistry Is Highly Correlated with NTRK3 Gene Rearrangements in Salivary Gland Tumors. Am J Surg Pathol 2021. https://doi.org/10.1097/PAS.0000000000001718.

[25] Hung YP, Jo VY, Hornick JL. Immunohistochemistry with a pan-TRK antibody distinguishes secretory carcinoma of the salivary gland from acinic cell carcinoma. Histopathology 2019. https://doi.org/10.1111/his.13845.

[26] Rudzinski ER, Lockwood CM, Stohr BA, Vargas SO, Sheridan R, Black JO, et al. Pan-Trk Immunohistochemistry Identifies NTRK Rearrangements in Pediatric Mesenchymal Tumors. Am J Surg Pathol 2018;42:927–35. https://doi.org/10.1097/PAS.0000000000001062.

[27] Hechtman JF, Benayed R, Hyman DM, Drilon A, Zehir A, Frosina D, et al. Pan-Trk Immunohistochemistry Is an Efficient and Reliable Screen for the Detection of NTRK Fusions. Am J Surg Pathol 2017;41. https://doi.org/10.1097/PAS.0000000000000911.

[28] Nguyen L, Chopra S, Laskar DB, Rao J, Lieu D, Chung F, et al. NOR-1 distinguishes acinic cell carcinoma from its mimics on fine-needle aspiration biopsy specimens 2020;102:1–6. https://doi.org/10.1016/j.humpath.2020.05.001.

[29] Wong KS, Mariño-Enriquez A, Hornick JL, Jo VY. NR4A3 Immunohistochemistry Reliably Discriminates Acinic Cell Carcinoma from Mimics. Head Neck Pathol 2021;15:425–32. https://doi.org/10.1007/s12105-020-01213-4.

[30] Millan N, Tjendra Y, Zuo Y, Jorda M, Garcia-Buitrago M, Velez-Torres JM, et al. Utility of NR4A3 on FNA cytology smears and liquid-based preparations of salivary gland. Cancer Cytopathol 2022. https://doi.org/10.1002/cncy.22632.

[31] Krishnan V, Nguyen L, Shen R, Lieu D, De Peralta-Venturina M, Fan X. NOR-1 (NR4A3) immunostaining on cytologic preparations for the preoperative diagnosis of acinic cell carcinoma of the salivary gland. J Am Soc Cytopathol 2022. https://doi.org/10.1016/j.jasc.2022.07.001.

[32] Le Guellec S, Velasco V, Pérot G, Watson S, Tirode F, Coindre JM. ETV4 is a useful marker for the diagnosis of CIC-rearranged undifferentiated round-cell sarcomas: A study of 127 cases including mimicking lesions. Mod. Pathol., vol. 29, 2016, p. 1523–31. https://doi.org/10.1038/modpathol.2016.155.

[33] Kuo Y, Lewis JS, Truong T, Yeh Y, Chernock RD, Zhai C, et al. Nuclear expression of AFF2 C-terminus is a sensitive and specific ancillary marker for DEK::AFF2 carcinoma of the sinonasal tract. Mod Pathol 2022;35:1587–95. https://doi.org/10.1038/s41379-022-01117-4.

[34] Freiberger SN, Brada M, Fritz C, Höller S, Vogetseder A, Horcic M, et al. SalvGlandDx – a comprehensive salivary gland neoplasm specific next generation sequencing panel to facilitate

diagnosis and identify therapeutic targets. Neoplasia (United States) 2021;23:473–87. https://doi.org/10.1016/j.neo.2021.03.008.

[35] Hernandez-Prera JC. Historical Evolution of the Polymorphous Adenocarcinoma. Head Neck Pathol 2019;13:415–22. https://doi.org/10.1007/s12105-018-0964-9.

[36] Sun T, Akalin A, Dresser K, Fischer AH, Zuo T. The Utility of MYB Immunohistochemistry (IHC) in Fine Needle Aspiration (FNA) Diagnosis of Adenoid Cystic Carcinoma (AdCC) 2021;15:389–94. https://doi.org/10.1007/s12105-020-01202-7.

[37] Poling JS, Yonescu R, Subhawong AP, Sharma R, Argani P, Ning Y, et al. MYB Labeling by Immunohistochemistry is More Sensitive and Specific for Breast Adenoid Cystic Carcinoma than MYB Labeling by FISH. Am J Surg Pathol 2017;41:973–9. https://doi.org/10.1097/PAS.0000000000000878.

[38] Moon A, Cohen C, Siddiqui MT. MYB expression: Potential role in separating adenoid cystic carcinoma (ACC) from pleomorphic adenoma (PA) 2016;44:799–804. https://doi.org/10.1002/dc.23551.